

Stress wave emission and plastic work of notched specimens

K. ISHIKAWA*, H. C. KIM

Department of Physics, Chelsea College, University of London, UK

The stress wave energy released from notched specimens of structural steel was measured in order to compare it with the recently proposed J -integral which takes account of the effect of large plastic deformation around the crack tip in ductile materials. Very close agreement was observed between the J -integral and the differential stress wave energy released. This suggests that the increment of the stress wave energy released is proportional to the decrement of the work done on the specimen during tensile testing under the plane stress condition.

This result, combined with information obtained from linear elastic fracture mechanics, leads to a relationship between the differential stress wave energy released and the stress intensity factor K , $[d(\text{SWER})/da] \propto K^2$. It was also found that in the region before general yielding, the stress wave energy release was proportional to the development of plastic zone size. A larger portion of the accumulated stress wave energy released was generated after general yielding due to void formation and coalescence. The accumulated stress wave energy released at the catastrophic crack growth point reached virtually the same value for each specimen, independent of the initial crack length. This implies that void formation and coalescence are not influenced by the initial crack length, but by the geometry of the crack tip.

1. Introduction

Stress wave emission is a form of energy release which is detected at the surface of a material undergoing deformation or fracture. In recent years a considerable amount of work has been done using this technique to examine crack growth, detect flaws and locate local transient instabilities in stressed structures in order to predict imminent criticality. Apart from these engineering applications, stress wave emission is of considerable interest in material science, since it can supply unique information about transient processes as they occur, e.g. slip events, twin formation and phase transformation. However, although these phenomena are intimately connected with basic processes in materials, relatively little work has so far been done to gain a fundamental aspect of stress wave emission.

To date, the primary characteristic parameters in the evaluation of stress wave emission activity have been wave form analysis, frequency spectrum, amplitude, the total number of counts from a wave ring-down, amplitude distribution

and the count rate. Among these, the total number of counts and the count rate are the most widely used and these have been correlated with applied stress, strain and stress intensity factor. In this paper we have taken a criterion for the stress wave emission activity which is different from those mentioned above, but one which previously has shown encouraging agreement with various mechanical properties in carbon epoxy composites [1, 2]. The relationship between these different criteria of stress wave emission activity will be briefly discussed.

The present work was carried out to compare the stress wave energy released from notched specimens of structural steel under the plane stress condition with the recently proposed J -integral [3, 4], which takes account of the effect of large plastic deformation around the crack tip in ductile materials.

2. J -integral as a measure of plastic work done around the notch-tip

The classical theory gives the critical surface energy for the crack growth of pure brittle

*On leave of absence from the National Research Institute for Metals, Tokyo, Japan.

materials which show no plastic work prior to fracture [5] and developments of a linear elastic fracture mechanics approach shows that the effective surface energy is equivalent to fracture toughness G . However, this linear elastic fracture mechanics approach imposes a restriction in that the analysis is only applicable in the elastic region, therefore it is impossible to apply it to ductile material or small specimens which show fairly large plasticity (non-linearity in the stress-strain relation and work-hardening before crack growth).

As a new criterion for the initiation of crack growth, the J -integral was proposed by Rice [3]. According to this theoretical approach, the J -integral is defined as the potential energy difference, p , of the stressed materials with a crack lengths a and $(a + \Delta a)$

$$J = - \frac{\Delta p}{\Delta a} \quad (1)$$

In particular, the J -integral for elastic material can be reduced to the fracture toughness, $G = J = K^2/E$, where K is the stress intensity factor and E is Young's Modulus. Furthermore, for rigid plastic material (non-work-hardening) J has been proved to be linearly proportional to the displacement [4]. The usefulness of the J -integral for work-hardening materials has not been theoretically substantiated yet. Nevertheless, experiments by Landes and Begley have successfully demonstrated that the path independent potential energy of the J -integral is an effective criterion for the initiation of crack growth of fully plastic, low and intermediate strength steels [6]. In this work, the potential energy p was replaced by the plastic work done during loading to a given displacement and measured by integrating the area under the load-deflection (displacement) curves.

According to their results, the critical J -integral was not influenced by the specimen geometry, but turned out to be constant within a scatter of less than $\pm 8\%$.

3. Experimental

3.1. Materials and mechanical test

The material used in this work was a low carbon-manganese structural steel, British Standard En 2. All specimens were cut from as-received plate. The dimensions of a double notched tensile specimen are shown in Fig. 1. The tensile direction was taken parallel to the rolling direction of the plate, and the crack lengths used were 1.5,

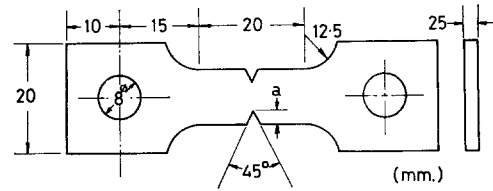


Figure 1 The dimensions of the notched specimen.

2.5 and 3.5 mm. The radius of the notch tip was 0.25 mm. After machining, all the specimens were chemically polished and subsequently a stress-relieving treatment was given for one hour at 550°C in the vacuum furnace (1×10^{-5} mm Hg) then furnace cooled. The microstructure of the specimen showed the ferrite-pearlite structure with an average grain diameter of ferrite about 0.03 mm. The main mechanical properties with an unnotched specimen are as follows, yield stress $\sim 33.6 \text{ kg mm}^{-2}$, ultimate tensile stress $\sim 58.0 \text{ kg mm}^{-2}$ and fracture strain ~ 0.16 .

Tensile testing was carried out on an Instron TT-DM, 5 ton load cell with a constant cross-head speed of 0.2 mm min^{-1} at room temperature. The displacement was measured along the parallel part of the specimen with a gauge length of 20 mm.

3.2. Stress wave emission measurement

A block diagram of the stress wave emission detection system used in this work is shown in Fig. 2. The stress wave pulses were detected by a DJB 645 transducer which has three main

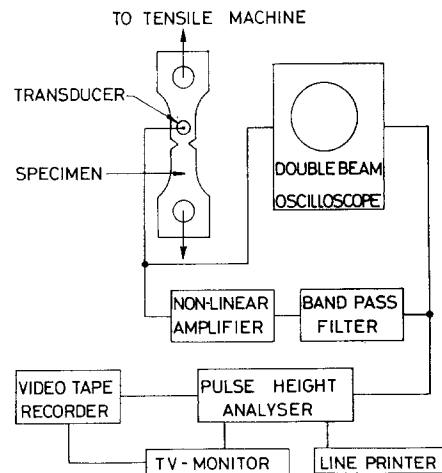


Figure 2 Block diagram of the apparatus used for this investigation.

resonant frequencies of 150, 170 and 200 kHz. This was attached to the specimen surface using an Acoustic Couplant (ACV-9, Dunegan Co, U.S.A.) and held in position by a constant load (0.67 kg) steel spring.

The output from the transducer was fed into a non-linear amplifier, with a delay time system so that only the first half-wave of the pulse height would be registered by the pulse height analyser. This delay time operates in a similar manner to a simple gating system with the first half cycle of the pulse being passed while the remaining part of the wave is blocked over a pre-determined period.

The input pulses to the pulse height analyser are sorted according to amplitude, and counts of the number of pulses in each of the 200 amplitude ranges are kept in core memory. The content of this memory is continuously displayed on a TV monitor. At the end of a run, the data on the channels are printed out by a digital parallel printer. Comprehensive details of this system will be published elsewhere [14].

Differentiation between the stress wave emission from the shoulder parts of the specimen and that emitted from the gauge length during test is difficult but it may be solved in the following way. Prior to mounting on to the testing machine, Hounsfield strip chucks were used to accommodate the specimen in such as way as to lock a particular area for pre-stressing.

This procedure utilizes the well-known Kaiser effect [7], when the testing of the specimen stress in the shoulder will cause only negligible extraneous noise.

4. Results

The typical stress displacement curves for three crack lengths of 1.5, 2.5 and 3.5 mm are shown in Fig. 3. Here, the stress referred to is the gross stress, i.e. the load divided by the unnotched cross-sectional area. The specimen with the longer crack length showed a lower stiffness, a lower general yield and fracture stress, and smaller elongation to the fracture. The fracture stress is regarded as the stress at which unstable crack growth takes place. The plastic deformation is mostly confined to the net area between the notches and this is confirmed by subsequent measurement after testing.

Previously, the stress wave energy released (SWER), E_s was given as

$$E_s = \sum N_i V_i^2 \quad (2)$$

where N_i is the number of emission events of amplitude level V_i , and was drawn on a logarithmic scale [1, 2]. However, in this work, as the testing material showed so little emission activity, the results (except for Fig. 4) are presented on a linear scale. In Fig. 4, and from now on, each datum point represents an average

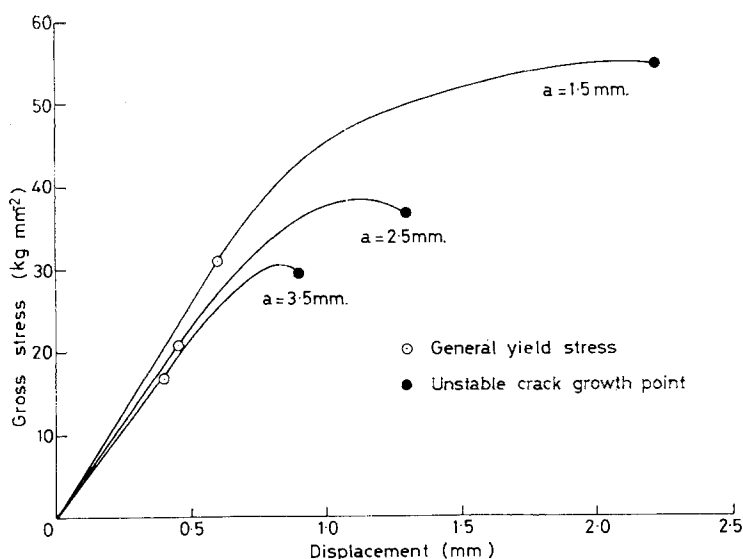


Figure 3 A set of stress displacement curves for the notched specimens.

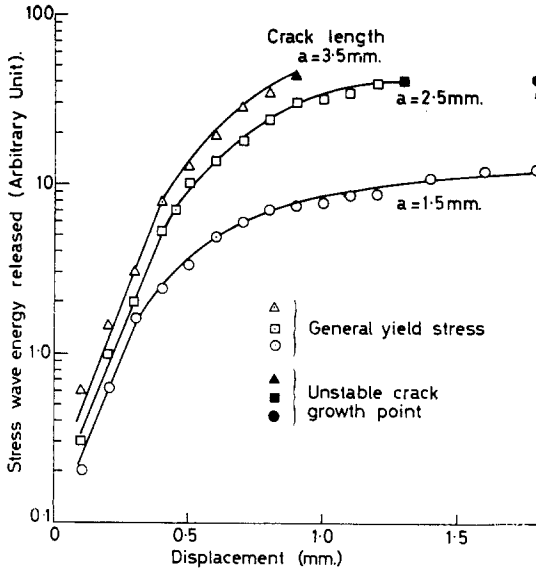


Figure 4 The change of stress wave energy released against displacement.

value from five different samples taken for each crack length.

The SWER of the specimen with a longer crack length is larger than that with a shorter one, which implies that the emission is proportional to the stress intensity factor raised to a certain power. This observation confirms the work of Dunegan *et al* on various structural materials using a different criterion of stress wave emission activity, the ring-down count [8], where an emission is recorded each time the stress wave signal exceeds the threshold voltage at which the counter is set.

The most interesting observation of this result is that the accumulated SWER at the fracture stress, for the different crack lengths where unstable crack growth is expected, fell at the same value.

To calculate the *J*-integral experimentally, Landes and Begley's procedure [6] was adopted. The load displacement curves are integrated graphically and the work done for a given displacement plotted as a function of crack length for each displacement in Fig. 5 The *J*-integral, from the definition as seen in Equation 1, is the negative of the slope of the plots in Fig. 5. In this case the real *J*-integral is a half of the slope because of the presence of two crack tips.

In the present work the SWER at a given displacement is assumed to be proportional to the work done on the specimen and is plotted in

Fig. 6 as a function of crack length for each displacement. In contrast to the slope in Fig. 5 the slopes in Fig. 6 are positive. We define this slope, which is the change of SWER with crack length, to be the differential SWER which may then be compared with the *J*-integral.

5. Discussion

The *J*-integral and differential SWER from the tensile test of the specimen with a crack length of 2.5 mm are plotted in Fig. 7. Before general yielding, the *J*-integral followed a square law with the displacement as predicted by the theory for linear elastic or small scale yielding materials and after yielding followed a linear relationship with displacement, as predicted by the theory for fully plastic materials [9].

It can be seen from Fig. 7 that the differential SWER follows the *J*-integral variation with displacement very closely. Therefore, we can write,

$$\frac{\Delta(\text{SWER})}{\Delta a} \propto J \left(= -\frac{\Delta p}{\Delta a} \right) \quad (3)$$

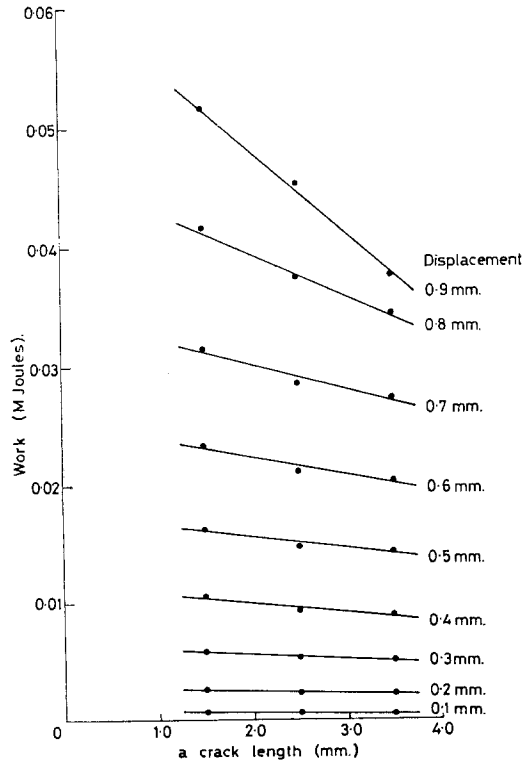


Figure 5 Work to a fixed displacement against crack length for cracked specimens.

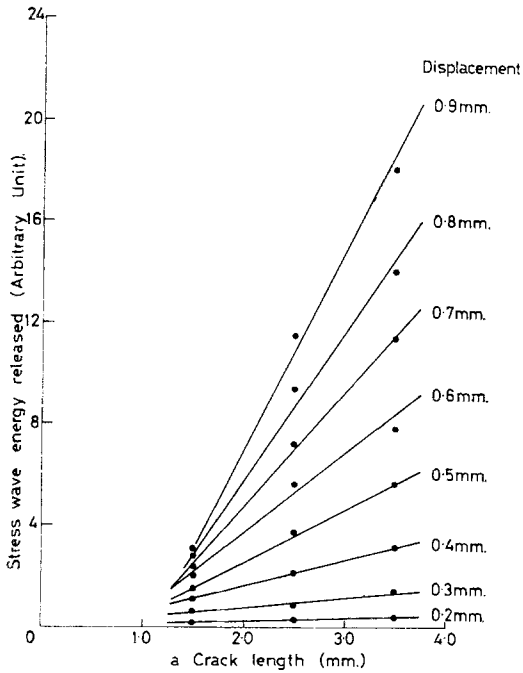


Figure 6 Stress wave energy released against crack lengths.

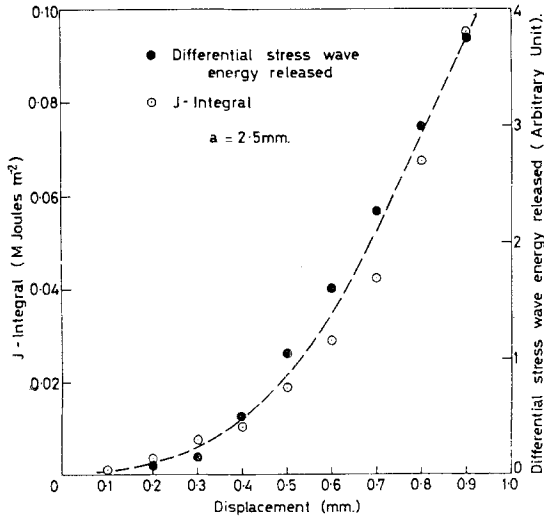


Figure 7 J-integral and differential stress wave energy released versus displacement for cracked specimens.

that is, the decrement of the plastic work done on the specimen is proportional to the increment of the SWER. This conclusion agrees with the original assumption made by Gerberich and Hartbower [10] in their investigation of the stress wave emission during slow crack growth for various materials. They postulated that the energy of the stress wave is some proportion of the available elastic energy and that this

stress wave energy is proportional to the square of the amplitude of the wave, $U \propto g^2$ where U is the strain energy released.

However, no satisfactory relationship was found experimentally between incremental crack growth and $\sum g^2$, therefore, $\sum g^2$ was replaced by $(\sum g)^2$ in their semi-empirical equation, $\Delta A \sim (\sum g)^2 E/K^2$ where ΔA is the incremental area swept by the crack. $\sum g$ is the sum of the stress wave amplitudes associated with that increment of growth, E is Young's modulus and K is the stress intensity factor. By this replacement their equation lost its physical meaning due to the cross-term in the $(\sum g)^2$ factor.

Furthermore, Equation [3] gives the relationship between the differential SWER and the stress intensity factor K , within the linear elastic region, where, $J = G = K^2/E$, is valid. Consequently, we can re-write Equation 3 for constant crack length,

$$SWER \propto K^2 \tag{4}$$

Dunegan *et al* [8] gives the relationship between the acoustic emission activity, in terms of total number of emission counts $\sum N$ from their ring-down count method and the stress intensity factor K , assuming that the acoustic emission count is proportional to the rate of increase of the volume of the plastic zone, as,

$$\sum N \propto K^m \tag{5}$$

where m is a constant varying between 2 and 8. If some universal relationship exists between SWER and the total count of Dunegan *et al*, we can write, from Equations 4 and 5,

$$(SWER)^{m/2} \propto \sum N. \tag{6}$$

By taking $m = 4$, Equation 6 will result in $(SWER)^2 \propto \sum N$, or by taking $m = 2$, as Palmer and Heald did [11], we obtain $(SWER) \propto \sum N$.

In the present work, the SWER is plotted against the plastic zone length, calculated using Bilby and Swinden's method [12], in Fig. 8. The SWER is linearly proportional to the plastic zone length before the general yielding, but the rate of increment varied with the initial crack length, being higher for the longer initial crack length. This can be explained by the difference in the broadening of the plastic zone, and the severe inter-action between the two plastic zones, resulting in the difference in the energy densities for different crack lengths.

Finally, we shall consider the micromechanism which is responsible for generation of stress

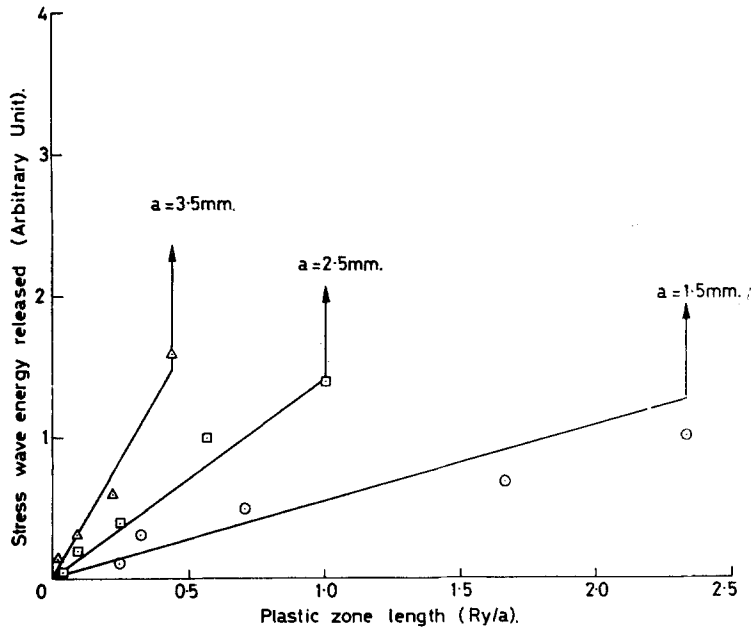


Figure 8 Stress wave released versus plastic zone length normalized with respect to crack length.

wave emission in steel. As mentioned previously, we found that before the general yielding the SWER comes from the plastic zones ahead of the crack tips; however, the larger portion of the SWER is produced after general yielding. This may be associated with void formation and coalescence. First, the plastic deformation and the strain concentration around the second phase takes place, then the weak particles or the weak interfaces will fail and as a result many voids are produced which then link up as the stress is increased. When void coalescence takes place catastrophically, the specimen will have reached an unstable crack growth point. At this point, the accumulated SWER of the three different crack length specimens reached almost the same value. This implies that the void coalescence which takes place mainly around the notch tips, is influenced by the radius of the crack tips and not by the crack lengths. This conclusion is confirmed by the optical micrographs of fracture surface by Smith and Knott [13], in which they show that ductile crack growth is always preceded by dimple rupture involving void coalescence.

6. Conclusions

1. Very good agreement was observed between the J -integral and the differential stress wave

energy released for a small size steel specimen under plane stress condition.

2. According to the above result it can be concluded that the increment of the stress wave energy released is proportional to the decrement of the potential energy of the specimen.

3. Before the general yielding, where $[\Delta(\text{SWER})/\Delta a] \propto K^2$ holds, the stress wave energy released is linearly proportional to the plastic zone length; however, the rate of increment is higher for the longer initial crack.

4. A larger portion of the stress wave energy released over the whole test appeared after general yielding; this may have been due to void formation and coalescence.

5. The accumulated stress wave energy released up to the beginning of the catastrophic growth of the crack reached almost the same value independent of crack length, which implies that void coalescence and formation are not influenced by the crack length, but by the radius of the crack tip.

Acknowledgements

This work was completed as part of a project to investigate the fundamental aspects of stress wave emission from solid under the support of the S.R.C. The authors wish to thank D. E. C. Elvin and J. W. Noad for assistance in the course

of this work. One of the authors (K.I.) gratefully acknowledges the financial support of the Science and Technology Agency of Japan.

References

1. H. C. KIM, A. P. RIPPER NETO and R. W. B. STEPHENS, *Nature, Physical Science* **237** (1972) 78.
2. *Idem, ibid* **241** (1973) 68.
3. J. R. RICE, *J. Appl. Mech.* **35** (1968) 379.
4. *Idem*, 'Fracture' (edited by H. Liebowitz) Vol. 2 (Academic Press, New York, 1968) p. 191.
5. A. A. GRIFFITH, *Phil. Trans. Roy. Soc.* **A221** (1921) 163.
6. J. D. LANDES and J. A. BEGLEY, ASTM STP 541 (1972) 24.
7. J. KAISER, *Arkiv för Eisenhüttenw.* **24** (1953) 43.
8. H. L. DUNEGAN, D. O. HARRIS and C. A. TATRO, *Eng. Fract. Mech.* **1** (1968) 105.
9. R. J. BUCCI, P. C. PARIS, J. D. LANDES and J. R. RICE, ASTM STP (1972) 40.
10. W. W. GERBRICH and C. E. HARTBOWER, *Int. J. Fract. Mech.* **3** (1963) 185.
11. I. G. PALMER and P. T. HEALD, *Mater. Sci. Eng.* **11** (1973) 181.
12. B. A. BILBY and K. H. SWINDEN, *Proc. Roy. Soc. (Lond.)* **A285** (1965) 23.
13. R. F. SMITH and J. F. KNOTT, Proc. Conf. on Application of Fracture Mechanics to Pressure Vessel Technology (Institution of Mechanical Engineers, London, 1971) p. 65.
14. H. C. KIM, to be published.

Received 21 September and accepted 31 December 1973.